

1 Onset of long-lived silicic and alkaline magmatism in eastern
2 North America preceded Central Atlantic Magmatic Province
3 emplacement

4 Sean T. Kinney¹, Scott A. MacLennan², Dawid Szymanowski³, C. Brenhin Keller⁴, Jill A.
5 VanTongeren⁵, Jacob B. Setera⁶, Steven J. Jaret⁷, C. Forrest Town⁴, Justin V. Strauss⁴,
6 Dwight C. Bradley⁴, Paul E. Olsen¹, Blair Schoene³

7 ¹*Lamont-Doherty Earth Observatory, Palisades, New York 10964, USA.*

8 ²*Department of Geosciences, University of Arizona, Tucson, Arizona 85721, USA.*

9 ³*Department of Geosciences, Princeton University, Princeton, New Jersey 08544, USA.*

10 ⁴*Department of Earth Science, Dartmouth College, Hanover, New Hampshire 03755, USA.*

11 ⁵*Tufts University Department of Earth and Ocean Sciences, Medford, Massachusetts 02155,*
12 *USA.*

13 ⁶*CASSMAR, University of Texas at El Paso – Jacobs JETS Contract, NASA Johnson Space*
14 *Center, Houston, TX 77058, USA.*

15 ⁷*American Museum of Natural History, New York, New York 10024, USA.*

16

17 **ABSTRACT**

18 The White Mountain Magma Series (WMMS) is the largest Mesozoic felsic igneous
19 province on the Eastern North American Margin (ENAM). Existing geochronology has
20 suggested that magmatism occurred over 50 Myr with published ages for the oldest units
21 apparently coeval with the ca. 201 Ma Central Atlantic Magmatic Province (CAMP), the flood
22 basalt province associated with the end-Triassic mass extinction and the opening of the Atlantic

23 Ocean. We use zircon U-Pb geochronology to show that emplacement of WMMS plutons was
24 already underway at 207.5 Ma. The largest volcanic-plutonic complex, the White Mountain
25 Batholith, was emplaced episodically from ca. 198.5 Ma to ca. 180 Ma, ca. 25 Myr older than
26 published ages suggest, and all samples we dated from the Moat Volcanics are between ca. 185
27 to 180 Ma. This result shows that the Moat Volcanics and the White Mountain Batholith are
28 broadly comagmatic, and it also constrains the age of a key Jurassic paleomagnetic pole. Our
29 data suggest that a regional mantle thermal anomaly in eastern North America developed at least
30 ca. 5 Myr prior to the main stage of CAMP flood basalt volcanism and suggests a geodynamic
31 link between the WMMS and the CAMP.

32 INTRODUCTION

33 Despite the long-recognized association of silicic magmatism with continental flood
34 basalts in large igneous provinces, constraints on the relative timing and the geodynamic
35 mechanisms that generate such events remains elusive (e.g., Bryan and Ferrari, 2013). The
36 CAMP, one of the largest continental flood basalt provinces (Marzoli et al., 2018; Marzoli et al.,
37 1999), was emplaced over a very brief time interval (< ca. 1 Myr) beginning at ca. 201.5 Ma and
38 coincided with the end-Triassic mass extinction (e.g., Blackburn et al., 2013; Davies et al.,
39 2017). The WMMS, a predominately silicic igneous province, is situated within the known field
40 of CAMP magmatism (McHone et al., 1987) (Fig. 1) and is the second-largest Mesozoic igneous
41 province in eastern North America. Published constraints based on whole rock and mineral K-
42 Ar, Ar-Ar, or Rb-Sr ages (Armstrong and Stump, 1971; Eby et al., 1992; Foland and Faul, 1977;
43 Foland et al., 1971) indicate an onset of magmatism at ca. 200 Ma, with episodic pulses
44 continuing for ca. 50 Myr. Recent zircon U-Pb studies of limited occurrence of Mesozoic
45 igneous rock (e.g., Eusden et al., 2017) and regional studies of detrital zircons from beach and

46 rivers sands (e.g., Bradley et al., 2015) have yielded no grains that suggest such a protracted
47 duration of magmatism.

48 Previous workers attributed WMMS magmatism to a variety of causal mechanisms,
49 including mantle plumes (e.g., Morgan, 1983), a long-lived thermal anomaly of unspecified
50 origin (e.g., Eby et al., 1992), and a ‘leaky’ transform fault (e.g., Bédard, 1985). Because the
51 existing chronology for the WMMS does not provide sufficient resolution to fully assess these
52 and other possibilities. We report new zircon U-Pb geochronology to date several WMMS units
53 that together constrain its onset, duration, and temporal relationship with CAMP magmatism.

54 **GEOLOGIC CONTEXT**

55 McHone and Butler (1984) divided all Mesozoic igneous rocks in northeastern North
56 America into four provinces: 1) The Coastal New England (CNE) Province; 2) The Eastern
57 North American Dolerite Province, now known as the CAMP; 3) The WMMS; and 4) The New
58 England Québec (NEQ) Province. The CNE province consists predominantly of basaltic dikes in
59 coastal Maine and has only one reliably dated unit, the intrusive Agamenticus intrusive complex
60 at 238.88 ± 0.11 Ma (Hussey et al., 2016). The NEQ province formed during an Early
61 Cretaceous episode of hotspot magmatism at ca. 125 Ma (Kinney et al., 2021).

62 The WMMS falls within the region of known CAMP dikes (Fig. 1) and consists of a
63 variety of volcanic and plutonic complexes, predominately ferroan (A_1 -type) granites (Eby,
64 1992; Frost and Frost, 2011) and minor silica-undersaturated intrusions (e.g., Creasy, 1989;
65 Henderson et al., 1989). Published whole rock ages suggest that early WMMS intrusions are
66 coeval with CAMP magmatism and continued until ca. 155 Ma (Table 1). The largest igneous
67 suite in the WMMS is a composite series of intrusions and volcanic rocks forming the White
68 Mountain Batholith (Fig. 2) with an apparent 50-Myr duration of magmatism (e.g., Eby et al.,

69 1992; Foland and Faul, 1977). Within the batholith, the Moat Volcanics unit has provided a key
70 Jurassic paleopole for constraining the apparent polar wander path of North America (Van
71 Fossen and Kent, 1990).

72 The zircon U-Pb geochronology reported here provides temporal constraints on the
73 relationship between CAMP and WMMS magmatism and specifically tests whether: 1)
74 magmatism in this province can be unambiguously temporally linked to the CAMP within a brief
75 temporal interval; or 2) magmatism is indeed protracted over a long timescale.

76 **METHODS**

77 We dated eleven samples via zircon U-Pb chemical abrasion-isotope dilution-thermal
78 ionization mass spectrometry (CA-ID-TIMS) and nine samples via zircon U-Pb laser ablation-
79 inductively coupled plasma-mass spectrometry (LA-ICP-MS) (Fig. 2). We selected samples with
80 previously published age constraints to capture the range of apparent magmatism within the
81 batholith. For CA-ID-TIMS measurements, we analyzed samples 2 – 5, where units have
82 published ages from ca. 201 – 195 Ma (Eby et al., 1992; Foland and Faul, 1977). Sample 16 is
83 from the unit (Conway Granite) with the youngest published age of entire province of ca. 155
84 Ma. We also sampled four units (samples 6, 8, 19, 20) based on published ca. 201 Ma ages
85 (Creasy, 1989; Eby et al., 1992; Foland and Allen, 1991; Henderson et al., 1989). We selected
86 two samples (14 and 15) from the Moat Volcanics at South Moat Mountain, where published
87 ages are between the oldest and youngest dated units within the White Mountain Batholith at ca.
88 173 – 167 Ma (Eby et al., 1992). Incidentally, these samples provide constraints on an important
89 Jurassic paleomagnetic pole (Van Fossen and Kent, 1990). Finally, we sampled the only
90 proximal zircon-bearing mafic unit (sample 1, 214 ± 9 Ma; Weston Geophysical Corporation,
91 1976) within the interval of WMMS magmatism. Samples dated via LA-ICP-MS additionally

92 targeted units with observable contact relationships within the Moat Volcanics and western
93 batholith.

94 Because of the large dispersion relative to analytical precision of single grain U-Pb dates
95 in each sample dated via CA-ID-TIMS, they likely record the timescale of crystallization for
96 zircon within each magmatic system. The calculation of a weighted mean age for such samples
97 requires subjective criteria for grain selection and leads to an age interpretation with ambiguous
98 geologic significance. Instead, we employed a modified Bayesian Markov Chain Monte Carlo
99 (MCMC) model (e.g., Keller et al., 2018; Kinney et al., 2021; Ratschbacher et al., 2018) that
100 more objectively estimates the timing of emplacement based on when the melt reaches
101 rheological lockup. We applied a similar approach to samples dated via LA-ICP-MS and report
102 ages that correspond to the *end* of zircon crystallization.

103 Sample numbers in the text were changed from field-IDs for brevity and are numbered in
104 order as projected along a W-E transect across the batholith. See Table DR1 and the GSA Data
105 Repository¹ for full sample descriptions, field-IDs, analytical methods, and description of U-Pb
106 age interpretations. Sample 21 is from the Agamenticus complex, dated by Hussey et al. (2016).

107 **RESULTS**

108 Four samples from the WMMS yielded ages from 210 to 200 Ma (Fig. 2), revealing an
109 apparently early episode of magmatism in the region that does not clearly fit into the known
110 ranges of either the CNE or WMMS provinces (Fig. 3). These are the relatively small plutons of
111 West Rattlesnake Mountain (sample 6; 207.24 +0.41/-0.27 Ma), Red Hill (sample 8; 203.86
112 +0.18/-0.12), Conway Granite at Whaleback (sample 19; 207.41 +0.05/-0.07 Ma), and
113 Rattlesnake Mtn. (sample 20; 200.76 +0.15/-0.08 Ma). These localities have typically been
114 associated with the WMMS based on previously published ages, and our work demonstrates that

115 their emplacement either clearly precedes (samples, 6, 8, 19), or is coincident with, the CAMP
116 (sample 20).

117 Magmatism within the White Mountain Batholith began no later than $198.56 \pm 0.42/-0.46$
118 Ma (samples 2, 5) and continued until ca. 190 Ma (samples 3, 4, 5, 7) with the emplacement of
119 large bodies of biotite granite that underlie most of the western batholith. In the eastern batholith,
120 the youngest (ca. 155 Ma) biotite granite (Sample 16) according to a previous K-Ar date (Eby et
121 al., 1992) has a U-Pb emplacement age of $182.31 \pm 0.30/-0.29$ Ma, which suggests that the
122 duration of magmatism within the White Mountain Batholith may be up to 25 Myr shorter than
123 previously thought. Sample 1, the only known WMMS gabbro with an original K-Ar age of ca.
124 215 Ma (Weston Geophysical Corporation, 1976), was dated herein via U-Pb at ca. $388.91 \pm$
125 4.98 Ma and likely belongs to the older New Hampshire Plutonic Suite (Dorais, 2003)

126 All the volcanic units (samples 11, 14, 15, 17, 18) from the Moat Volcanics and their
127 intrusive contacts (10, 12, 16), except for an anomalous sample (Sample 13) at 198.410 ± 0.097
128 Ma, were emplaced between ca. 185 - 180 Ma.

129 **DISCUSSION**

130 Predominately alkaline magmatism in the WMMS began at $207.41 \pm 0.05/-0.07$ Ma, ca. 6
131 Myr prior to the emplacement of the CAMP flood basalts elsewhere in the region. Significant
132 differences between the zircon U-Pb emplacement ages presented here and existing K-Ar and
133 Rb-Sr ages (Fig. 3) are present at many localities, and particularly, in the eastern batholith,
134 suggesting that thermal heating from either the spatially overlapping Cretaceous NEQ province,
135 a magmatic-hydrothermal event of an unknown age, or the effects of alteration or open system
136 behavior affected the minerals used for K-Ar or Rb-Sr dating in previous studies. The good
137 agreement of nearly all samples from the Moat Volcanics and associated intrusions suggest

138 emplacement from 185 – 180 Ma and that the ca. 198 Ma date reflects recycling of an older
139 WMMS xenolith in the system. These data merit closer scrutiny of the Moat Volcanics as a
140 reliable paleopole considering that the magnetizations for this locality are interpreted to be
141 secondary thermochemical remnant magnetizations (Van Fossen and Kent, 1990). Therefore, any
142 emplacement age only provides a maximum estimate for the timing of magnetization.

143 A similar analogue to our observations of this region on the ENAM is the Paraná-
144 Etendeka (P-E) flood basalt province, where existing geochronologic constraints demonstrate a
145 prolonged duration of intrusive silicic and alkaline magmatism spatially associated with flood
146 basalts (Gomes and Vasconcelos, 2021). In the P-E, small-scale alkaline magmatism both pre-
147 dates the eruption of flood basalts by ca. 4 Myr and post-dates the main phase of flood basalt
148 magmatism by as much as ca. 7 Myr. It is difficult to make direct comparisons to the CAMP and
149 the WMMS without reliable zircon U-Pb age constraints for both the P-E lavas themselves
150 (Rocha et al., 2020) or for the intrusive silicic-alkaline units associated with the P-E province
151 (e.g., the Damaraland Complexes). However, geodynamic models (e.g., Gibson et al., 2006) for
152 P-E magmatism suggest that the early production of silicic and alkaline melts, as well as their
153 duration are consistent with the combined effects of regional extension and the thermal
154 interaction of a plume head with thick, metasomatized continental lithosphere.

155 Like the P-E, Triassic-Jurassic ENAM magmatism is broadly associated with rifting of a
156 supercontinent, though no consensus exists on the specific geodynamic mechanism. CAMP
157 geochemistry largely points to a depleted upper mantle source for the widespread flood basalt
158 magmatism (e.g., Marzoli et al., 2018), whereas geochemistry from the WMMS (Eby et al.,
159 1992; Foland and Allen, 1991; Foland et al., 1988) suggests a mantle source with variable crustal
160 input but is insufficient to unambiguously characterize the source characteristics or degree of

161 fractionation and assimilation processes. A rift-related mechanism is consistent with the CNE
162 province for which there is evidence of magmatism at ca. 239 Ma (Hussey et al., 2016),
163 approximately coeval with the onset of sedimentation, and therefore extension, in ENAM rift
164 basins. Furthermore, because of the significant offset between zircon U-Pb and vintage K-Ar
165 dates from rocks in this region shown by this study and elsewhere (e.g., Hussey et al., 2016), the
166 only reliable estimate on the timing and duration of the CNE province is the 238.88 ± 0.11 Ma
167 age of the Agamenticus Complex (Sample 21) and there is insufficient evidence to suggest that
168 the ca. 207 Ma plutons dated here are related to this event. It therefore seems more likely that the
169 silicic magmatism at ca. 207 Ma was a precursor to flood basalt volcanism. Because there is no
170 evidence from ENAM rift basins that indicate changes in either regional stress states or extension
171 rates at ca. 207.5 Ma (e.g., Withjack et al., 2013), any proposed causal mechanism for the CAMP
172 should account for localized production of silicic and alkaline melts up to 6 Myr prior to the
173 main phase of flood basalt magmatism

174 **CONCLUSIONS**

175 We demonstrate that small-scale regional silicic and alkaline magmatism associated with
176 the WMMS began at ca. 207.5 Ma, which both post-dates the ca. 239 Ma CNE Province and pre-
177 dates the ca. 201.5 Ma CAMP. Beginning at ca. 198.5 Ma, the main phase of WMMS
178 magmatism, the White Mountain Batholith was episodically emplaced over ca. 20 Myr,
179 significantly shorter than previous estimates of 50 Myr. This discrepancy likely reflects post-
180 emplacement open system behavior in the K-Ar system. Zircon U-Pb age estimates of ca. 185 -
181 180 Ma for the Moat Volcanics provide a maximum constraint for the Jurassic paleopole derived
182 from this locality. The absence of evidence for any change in regional stress state or extension
183 rate in this segment of the ENAM at ca. 207.5 Ma suggests the development of a regional

184 thermal anomaly ultimately leading to the production of widespread flood basalt magmatism
185 may also be responsible for the onset of the WMMS.

186

187 **ACKNOWLEDGMENTS**

188 STK acknowledges support from: National Science Foundation Graduate Research Fellowship
189 Program DGE 16-44869; Earthscope Graduate Student Program in Geochronology supported
190 under NSF Grant Nos. EAR-1358514, 1358554, 1358401, 1358442, and 1101100; the LDEO
191 Chevron Student Initiative Fund; and a GSA graduate student research grant. Thanks to the
192 Arizona LaserChron Center (NSF-EAR 1649254) for assistance with LA-ICP-MS analyses. We
193 thank the White Mountain National Forest for land and vehicle access and Elaine Swett, Austin
194 Hart, Jenny Cramer, and Diana Kinney for assistance in the field. This paper benefitted from
195 discussion with Martha Withjack and Dennis Kent.

196

197 **FIGURES AND CAPTIONS**

198

199 **Figure 1.** A) Eastern North American Margin (ENAM) with estimated dike locations from
200 Withjack et al. (2013); study area is within black rectangle B) Study area; province boundaries
201 defined by western-most extent of dikes associated with the Central Atlantic Magmatic Province
202 (CAMP, black) and Coastal New England Province (CNE, Orange) defined by McHone and
203 Butler (1984). Considerable uncertainty is associated with the boundaries of each province
204 because they are defined by dike distributions, many without direct radiometric age constraints.
205 Rift basins containing the record of CAMP lava flows and intrusives on the ENAM and are
206 shown in black. Continental-scale dikes associated with the CAMP (McHone et al., 1987) shown

207 in blue. NYC – New York City; NB – Newark Basin; HB – Hartford Basin; CAMP – Central
208 Atlantic Magmatic Province; WMMS – White Mountain Magma Series; CNE – Coastal New
209 England; FB – Fundy Basin.

210

211 **Figure 2.** White Mountain Batholith with sample numbers used in text and preferred ages at the
212 95% credible interval for all CA-ID-TIMS and LA-ICP-MS samples. Superscripts refer to
213 method used: A, MCMC from LA-ICP-MS data; B, MCMC from CA-ID-TIMS data; C,
214 Weighted Mean (WM) from CA-ID-TIMS data. See the GSA Data Repository for sample
215 descriptions, detailed methods, and full model results.

216

217 **Figure 3.** (Top) Summary of preferred ages as shown in Fig. 2, where marker symbols
218 correspond to method and color corresponds to map unit. (Bottom) Kernel density of preferred
219 zircon U-Pb ages produced in this study and all published dates (K-Ar and Rb-Sr) from the
220 White Mountain Batholith and Coastal New England Province plutons (Creasy, 1989; Eby et al.,
221 1992; Foland and Allen, 1991; Foland and Faul, 1977; Henderson et al., 1989). Vertical red bar
222 for CAMP shows age range of all published zircon U-Pb ages (Blackburn et al., 2013; Davies et
223 al., 2017; Heimdal et al., 2018; Marzoli et al., 2019). Horizontal blue bar for CNE province dikes
224 shows approximate range of published K-Ar dates (McHone and Butler, 1984). Sample 21 is
225 Agamenticus Complex with zircon U-Pb date from Hussey et al. (2016).

226 TABLE CAPTIONS

227 **Table 1.** Zircon U-Pb ages showing sample numbers in Fig. 2. Mapped units in New Hampshire
228 from Lyons et al. (1997) and in Maine from Creasy (1989). Both Bayesian MCMC

229 emplacement/end-crystallization ages and weighted mean calculations are reported for all
230 samples.

231

232 [Please include this text at the end of your paper if you are including an item in the Data
233 Repository.]

234 ¹GSA Data Repository item 201Xxxx, Figures DR1 to DR 49 contain zircon images, Concordia
235 and weighted mean plots and the results of MCMC modeling; Tables DR1 to DR2 contain
236 detailed sample information and detailed methods for LA-ICP-MS analyses; Datasets DR1 to
237 DR3 contain whole rock chemistry and measured isotopic data for all samples, is available
238 online at www.geosociety.org/pubs/ft20XX.htm, or on request from editing@geosociety.org.

239 REFERENCES CITED

240 Armstrong, R. L., and Stump, E., 1971, Additional K-Ar dates, White Mountain magma series,
241 New England: American Journal of Science, v. 270, no. 5, p. 331-333.

242 Bédard, J. H., 1985, The Opening of the Atlantic, the Mesozoic New-England Igneous Province,
243 and Mechanisms of Continental Breakup: Tectonophysics, v. 113, no. 3-4, p. 209-232.

244 Blackburn, T. J., Olsen, P. E., Bowring, S. A., McLean, N. M., Kent, D. V., Puffer, J., McHone,
245 G., Rasbury, E. T., and Et-Touhami, M., 2013, Zircon U-Pb Geochronology Links the
246 End-Triassic Extinction with the Central Atlantic Magmatic Province: Science, v. 340,
247 no. 6135, p. 941-945.

248 Bradley, D. C., O'Sullivan, P., and Bradley, L. M., 2015, Detrital zircons from modern sands in
249 New England and the timing of Neoproterozoic to Mesozoic Magmatism: American
250 Journal of Science, v. 315, no. 5, p. 460-485.

251 Bryan, S. E., and Ferrari, L., 2013, Large igneous provinces and silicic large igneous provinces:
252 Progress in our understanding over the last 25 years: GSA Bulletin, v. 125, no. 7-8, p.
253 1053-1078.

254 Creasy, J. W., 1989, Geology and geochemistry of the Rattlesnake Mountain igneous complex,
255 Raymond and Casco, Maine, *in* Tucker, R. D., and Marvinney, R. G., eds., Studies in
256 Maine Geology: Volume 4 - igneous and metamorphic geology: Maine Geological
257 Survey, Volume 66, Maine Geological Survey Publications, p. 63-78.

258 Davies, J. H. F. L., Marzoli, A., Bertrand, H., Youbi, N., Ernesto, M., and Schaltegger, U., 2017,
259 End-Triassic mass extinction started by intrusive CAMP activity: Nature
260 Communications, v. 8, no. 1, p. 15596.

261 Dorais, M. J., 2003, The petrogenesis and emplacement of the New Hampshire plutonic suite:
262 American Journal of Science, v. 303, no. 5, p. 447-487.

263 Eby, G. N., 1992, Chemical subdivision of the A-type granitoids: Petrogenetic and tectonic
264 implications: Geology, v. 20, no. 7, p. 641-644.

265 Eby, G. N., Krueger, H. W., and Creasy, J. W., 1992, Geology, geochronology, and
266 geochemistry of the White Mountain batholith, New Hampshire, *in* Puffer, J. H., and
267 Ragland, P. C., eds., Eastern North American Mesozoic Magmatism, Volume 268,
268 Geological Society of America, p. 379-398.

269 Eusden, J. D., Hillenbrand, I. W., Baker, S., and Cargill, J. L., 2017, Bedrock Geologic Map of
270 the Jefferson, New Hampshire 7.5' Quadrangle, NH.

271 Foland, K. A., and Allen, J. C., 1991, Magma sources for Mesozoic anorogenic granites of the
272 White Mountain magma series, New England, USA: Contributions to Mineralogy and
273 Petrology, v. 109, no. 2, p. 195-211.

274 Foland, K. A., and Faul, H., 1977, Ages of the White Mountain intrusives; New Hampshire,
275 Vermont, and Maine, USA: *American Journal of Science*, v. 277, no. 7, p. 888-904.

276 Foland, K. A., Jiang-feng, C., Gilbert, L. A., and Hofmann, A. W., 1988, Nd and Sr isotopic
277 signatures of Mesozoic plutons in northeastern North America: *Geology*, v. 16, no. 8, p.
278 684-687.

279 Foland, K. A., Quinn, A. W., and Giletti, B. J., 1971, K-Ar and Rb-Sr Jurassic and Cretaceous
280 ages for intrusives of the White Mountain magma series, northern New England:
281 *American Journal of Science*, v. 270, no. 5, p. 321-330.

282 Frost, C. D., and Frost, R., 2011, On Ferroan (A-type) Granitoids: their Compositional
283 Variability and Modes of Origin: *Journal of Petrology*, v. 52, no. 1, p. 39-53.

284 Gibson, S. A., Thompson, R. N., and Day, J. A., 2006, Timescales and mechanisms of plume–
285 lithosphere interactions: $^{40}\text{Ar}/^{39}\text{Ar}$ geochronology and geochemistry of alkaline igneous
286 rocks from the Paraná–Etendeka large igneous province: *Earth and Planetary Science*
287 *Letters*, v. 251, no. 1, p. 1-17.

288 Gomes, A. S., and Vasconcelos, P. M., 2021, Geochronology of the Paraná-Etendeka large
289 igneous province: *Earth-Science Reviews*, v. 220, p. 103716.

290 Heimdal, T. H., Svensen, H. H., Ramezani, J., Iyer, K., Pereira, E., Rodrigues, R., Jones, M. T.,
291 and Callegaro, S., 2018, Large-scale sill emplacement in Brazil as a trigger for the end-
292 Triassic crisis: *Scientific Reports*, v. 8, no. 1, p. 141.

293 Henderson, C. M. B., Pendlebury, K., and Foland, K. A., 1989, Mineralogy and Petrology of the
294 Red Hill Alkaline Igneous Complex, New Hampshire, U.S.A: *Journal of Petrology*, v. 30,
295 no. 3, p. 627-666.

296 Hussey, A., Bothner, W., and Thompson, P., 2016, Bedrock geology of the Kittery 1: 100 000
297 quadrangle, southwestern Maine and southeastern New Hampshire. : Bulletin of the
298 Maine Geological Survey, v. 45, p. 99.

299 Keller, C. B., Schoene, B., and Samperton, K. M., 2018, A stochastic sampling approach to
300 zircon eruption age interpretation: *Geochemical Perspectives Letters*, p. Medium: ED;
301 Size: p. 31-35.

302 Kinney, S. T., MacLennan, S. A., Keller, C. B., Schoene, B., Setera, J. B., VanTongeren, J. A.,
303 and Olsen, P. E., 2021, Zircon U-Pb Geochronology Constrains Continental Expression
304 of Great Meteor Hotspot Magmatism: *Geophysical Research Letters*, v. 48, no. 11, p.
305 e2020GL091390.

306 Lyons, J. B., Bothner, W. A., Moench, R. H., and Thompson Jr, J. B., 1997, Bedrock geologic
307 map of New Hampshire.

308 Marzoli, A., Bertrand, H., Youbi, N., Callegaro, S., Merle, R., Reisberg, L., Chiaradia, M.,
309 Brownlee, S. I., Jourdan, F., Zanetti, A., Davies, J. H. F. L., Cuppone, T., Mahmoudi, A.,
310 Medina, F., Renne, P. R., Bellieni, G., Crivellari, S., El Hachimi, H., Bensalah, M. K.,
311 Meyzen, C. M., and Tegner, C., 2019, The Central Atlantic Magmatic Province (CAMP)
312 in Morocco: *Journal of Petrology*, v. 60, no. 5, p. 945-996.

313 Marzoli, A., Callegaro, S., Dal Corso, J., Davies, J. H. F. L., Chiaradia, M., Youbi, N., Bertrand,
314 H., Reisberg, L., Merle, R., and Jourdan, F., 2018, The Central Atlantic Magmatic
315 Province (CAMP): A Review, *in* Tanner, L. H., ed., *The Late Triassic World: Earth in a*
316 *Time of Transition*: Cham, Springer International Publishing, p. 91-125.

317 Marzoli, A., Renne, P. R., Piccirillo, E. M., Ernesto, M., Bellieni, G., and Min, A. D., 1999,
318 Extensive 200-Million-Year-Old Continental Flood Basalts of the Central Atlantic
319 Magmatic Province: *Science*, v. 284, no. 5414, p. 616-618.

320 McHone, J. G., and Butler, J. R., 1984, Mesozoic igneous provinces of New England and the
321 opening of the North Atlantic Ocean: *GSA Bulletin*, v. 95, no. 7, p. 757-765.

322 McHone, J. G., Ross, M. E., and Greenough, J. D., 1987, Mesozoic Dyke Swarms of Eastern
323 North America, *in* Halls, H. C., and Fahrig, W. H., eds., *Mafic dyke swarms: Geological*
324 *Association of Canada Special Paper 34*, p. 102-111.

325 Morgan, W. J., 1983, Hotspot tracks and the early rifting of the Atlantic: *Tectonophysics*, v. 94,
326 no. 1, p. 123-139.

327 Ratschbacher, B. C., Keller, C. B., Schoene, B., Paterson, S. R., Anderson, J. L., Okaya, D.,
328 Putirka, K., and Lippoldt, R., 2018, A New Workflow to Assess Emplacement Duration
329 and Melt Residence Time of Compositionally Diverse Magmas Emplaced in a Sub-
330 volcanic Reservoir: *Journal of Petrology*, v. 59, no. 9, p. 1787-1809.

331 Rocha, B. C., Davies, J. H. F. L., Janasi, V. A., Schaltegger, U., Nardy, A. J. R., Greber, N. D.,
332 Lucchetti, A. C. F., and Polo, L. A., 2020, Rapid eruption of silicic magmas from the
333 Paraná magmatic province (Brazil) did not trigger the Valanginian event: *Geology*.

334 Van Fossen, M. C., and Kent, D. V., 1990, High-latitude paleomagnetic poles from Middle
335 Jurassic Plutons and moat volcanics in New England and the controversy regarding
336 Jurassic Apparent Polar Wander for North America: *Journal of Geophysical Research*, v.
337 95, no. B11.

338 Weston Geophysical Corporation, 1976, Geologic Investigations, appendix G-6, Radiometric
339 Dating, Private Report BE-SG 7603, Weston Geophysical Corporation to Boston Edison
340 Company.

341 Withjack, M. O., Schlische, R. W., Malinconico, M. L., and Olsen, P. E., 2013, Rift-basin
342 development: lessons from the Triassic–Jurassic Newark Basin of eastern North America:
343 Geological Society, London, Special Publications, v. 369, no. 1, p. 301-321.

344

Figure 1

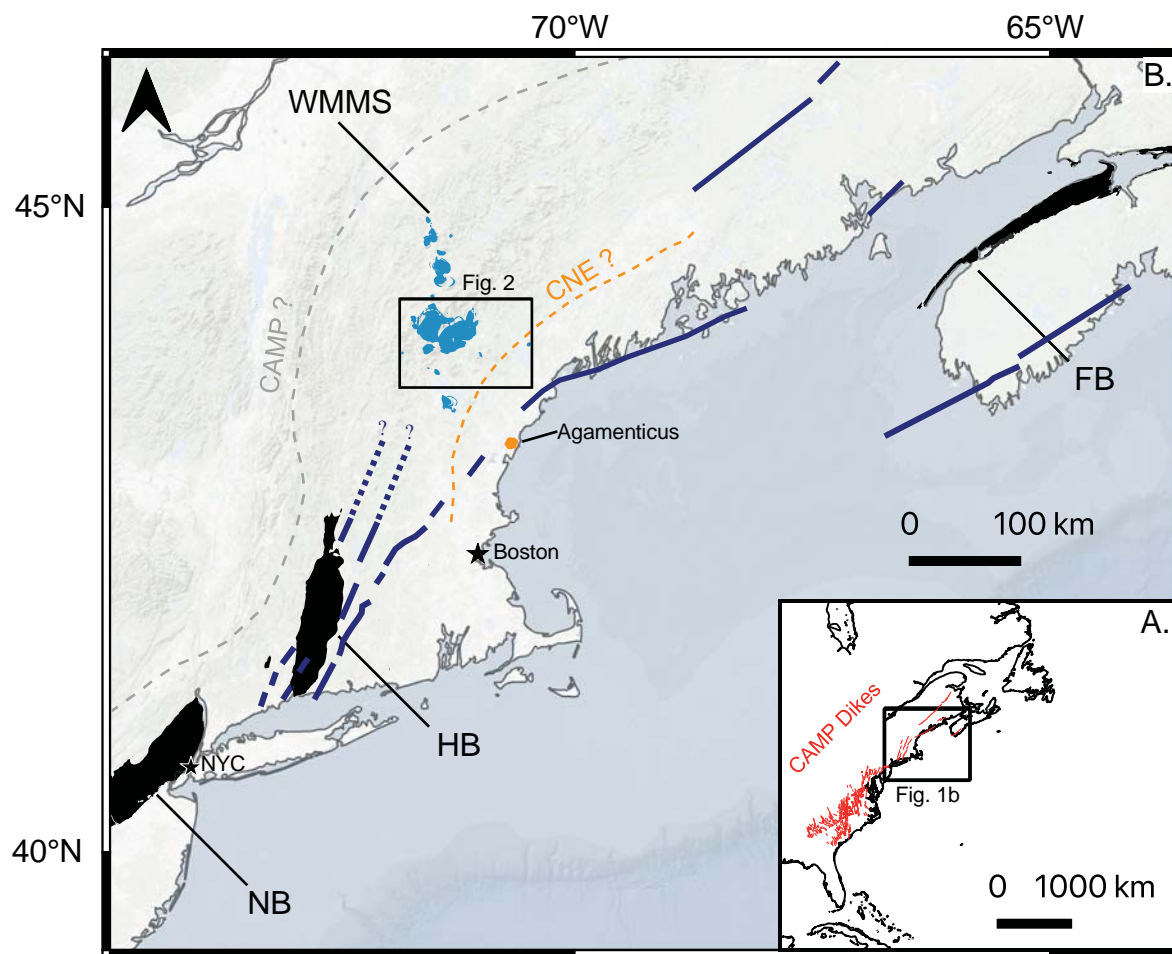


Figure 2

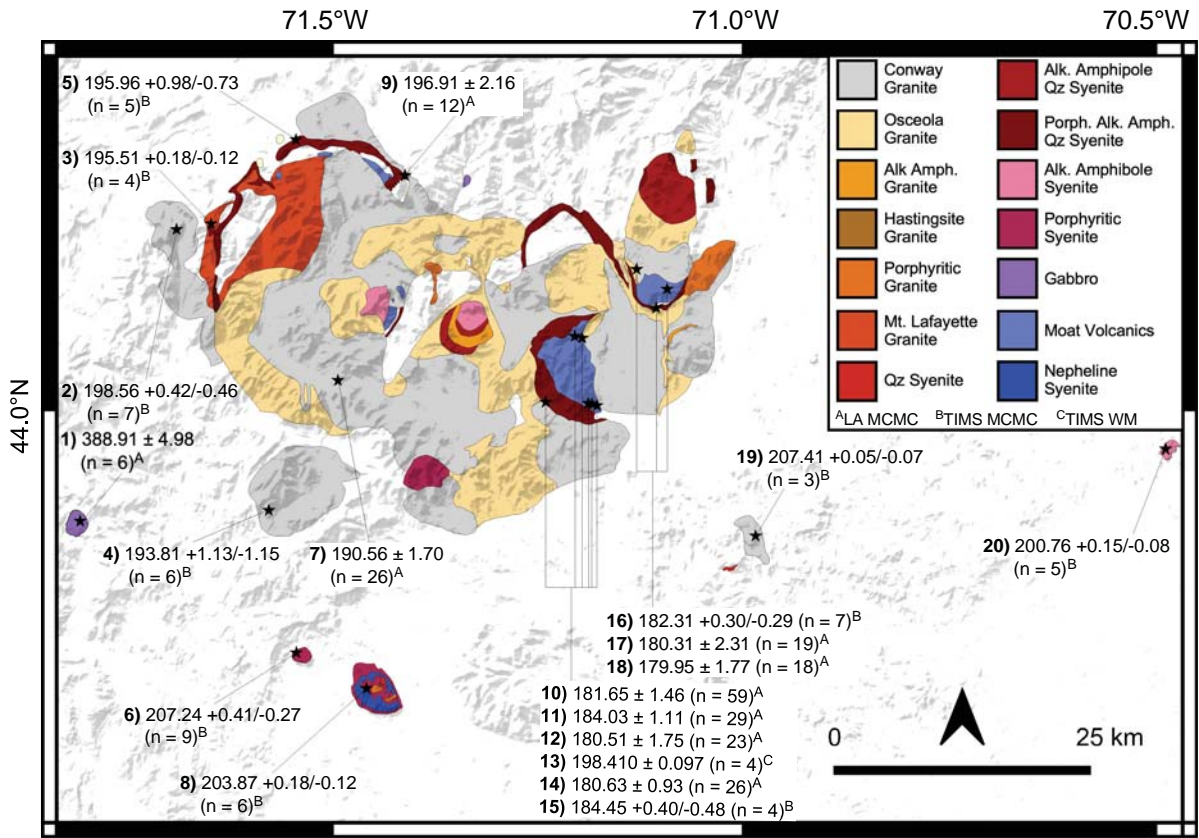


Figure 3

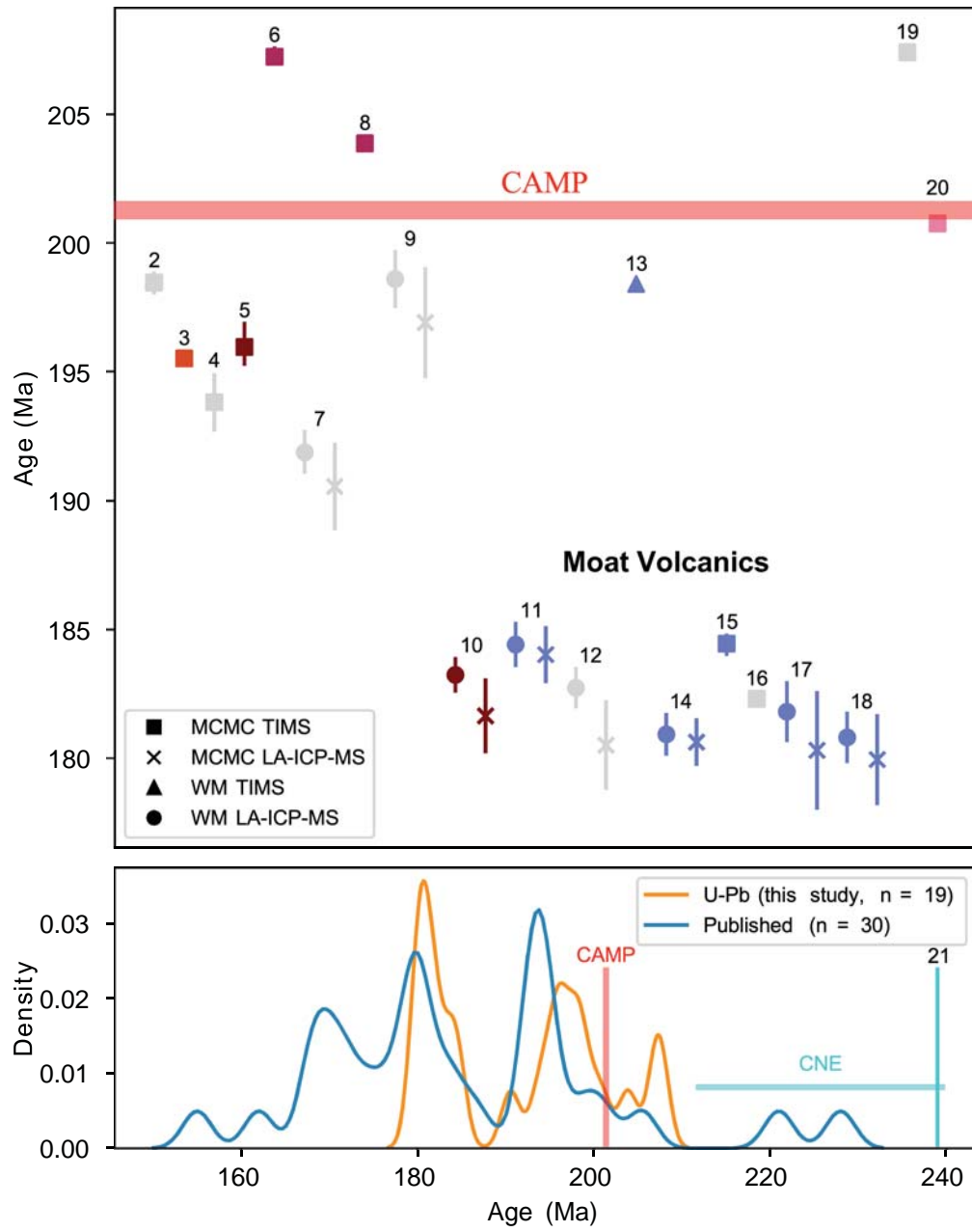


TABLE 1. SUMMARY OF ZIRCON U-PB AND PUBLISHED AGES

<i>Zircon U-Pb results</i>				
#	Weighed Mean (Ma)	MCMC (Ma)*	Method	Published Age (Ma)
1	393.55 ± 2.54 (MSWD = 3.42, n = 6)	388.91 ± 4.98	LA	215 ± 7 ¹
2	198.55 ± 0.11 (MSWD = 2.2, n = 3)	198.56 +0.42/-0.46	CA	198 ± 4 ² ; 194 ± 2 ³
3	195.494 ± 0.105 (MSWD = 0.35, n = 4)	195.51 +0.18/-0.12	CA	195 ± 6 ⁴
4	193.45 ± 0.11 (MSWD = 1.1, n = 3)	193.81 +1.13/-1.15	CA	186 ± 4; 184 ± 4; 193 ± 2
5	-	195.96 +0.98/-0.73	CA	193 ± 6 ⁴ ; 201 ± 6 ⁴
6	206.618 ± 0.033 (MSWD = 1.7, n = 7)	207.24 +0.41/-0.27	CA	198 ± 10 ³
7	191.89 ± 0.84 (MSWD = 1.55, n = 26)	190.56 ± 1.70	LA	184 ± 4 ^{2†}
8	203.733 ± 0.028 (MSWD = 1.2, n = 5)	203.87 +0.18/-0.12	CA	201.93 ± 1.64 ⁶
9	198.60 ± 1.13 (MSWD = 1.80, n = 12)	196.91 ± 2.16	LA	184 ± 4 ²
10	183.24 ± 0.70 (MSWD = 1.41, n = 59)	181.65 ± 1.46	LA	179 ± 4 ⁴
11	184.42 ± 0.88 (MSWD = 0.78, n = 29)	184.03 ± 1.11	LA	168.2 ± 1.2 ⁴
12	182.74 ± 0.81 (MSWD = 1.63, n = 23)	180.51 ± 1.75	LA	172 ± 3 ^{5†} ; 180 ± 2 ³
13	198.410 ± 0.097 (MSWD = 1.6, n = 4)	-	CA	173 ± 1.5 ⁴
14	180.93 ± 0.83 (MSWD = 0.48, n = 26)	180.63 ± 0.93	LA	173 ± 1.5 ⁴
15	184.29 ± 0.10 (MSWD = 0.32, n = 3)	184.45 +0.40/-0.48	CA	173 ± 1.5 ⁴
16	182.305 ± 0.089 (MSWD = 1.3, n = 7)	182.31 +0.30/-0.29	CA	155 ± 4 ⁴
17	181.81 ± 1.19 (MSWD = 1.61, n = 19)	180.31 ± 2.31	LA	173 ± 1.5 - 168.2 ± 1.2 ⁴
18	180.81 ± 1.00 (MSWD = 1.35, n = 18)	179.95 ± 1.77	LA	173 ± 1.5 - 168.2 ± 1.2 ⁴
19	207.418 ± 0.044 (MSWD = 0.74, n = 3)	207.41 +0.05/-0.07	CA	189 ± 4 ²
20	200.676 ± 0.021 (MSWD = 1.7, n = 5)	200.76 +0.15/-0.08	CA	205 ± 2 ⁷
21	238.88 ± 0.11 (MSWD = 1.4, n = 4) ^{8††}	-	CA	228 ± 5 ²

¹Weston Geophysical. ²Foland and Faul (1977). ³Foland and Allen (1991). ⁴Eby et al. (1992).

⁵Foland et al. (1971). ⁶Henderson et al. (1989). ⁷Creasy (1989). ⁸Hussey et al. (2016).

*MCMC age calculated using MELTS prior for samples dated via CA-ID-TIMS and using a generic, exponential prior for samples dated via LA-ICP-MS.

††Calculated from Hussey et al. (2016).